Understanding the Structural and Chemical Basis of Chalcopyrite Solar Cell Operation

DOE-AAT-1-30620-05

Principal Investigators: Angus Rockett, I. M. Robertson
Department of Materials Science and Engineering,
University of Illinois, Urbana IL 61801

Analysis of Results *vis a vis* Solar Cells

We have carried out a detailed electron microscopic analysis of Cu(In,Ga)Se_2 (CIGS) solar cell materials and obtained a range of results on the microstructure and microchemistry of complete devices and absorber layers. Our interpretation of the implications for solar cell operation ~~are~~ is described here.

Microstructure

We have examined both polycrystalline and single-crystal thin films of CIGS grown by a number of processes at a number of laboratories including Shell Solar Industries (SSI), Global Solar Energy (GSE), the University of Delaware Institute for Energy Conversion (IEC), the University of Illinois (UIUC), and the Hahn Meitner Institute (HMI). The materials produced in these laboratories are created by solid/liquid phase selenization, multisource evaporation, multisource evaporation, a hybrid sputtering and evaporation process, and MOVPE, respectively. The deposition temperatures varied from 400 (some IEC material) to 725°C (epilayers) and with most temperatures ranging from 550 to 650°C. Deposition rates ranged from >2 (SSI, GSE, IEC) to <0.2 (HMI) μm/hr. The epitaxial single crystals produce generally poor performance devices (4-8% efficient) while the polycrystalline materials studied yielded at least 10%-efficient solar cells uniformly. Consequently, the materials analyzed cover a very wide range of processing conditions. Despite this many common features were observed.

Grain size & twins:

There is no measurable effect of grain size on CIGS solar cells. This is in agreement with many experimental results obtained in the past 15 years. The TEM results simply confirm that the actual grain size is consistent with column sizes in most materials. Likewise, the long-standing results suggesting that twins are not a problem are in agreement with our data, which show no correlation of twin density with device performance. The only caveat concerning twins is that lower-temperature depositions result in far more twins and lower performances. However, the twin density also varies in devices of equivalent performance so any connection is weak at best.

Dislocations

Dislocations of all types were found to be generally rare in polycrystalline CIGS, presumably because the dislocations are sufficiently mobile at the deposition temperature to escape from the grains. Films deposited at low temperatures show reduced grain sizes and greatly increased twin densities but no dramatic increase in dislocation density. The only case in which dislocations are common is in epitaxial films where escape to grain boundaries is difficult or where misfit

dislocations occur. It may well be the case that the performance of the epitaxial devices is limited by dislocations but if so, this must be through the minority carriers rather than through the majority carriers. This conclusion is also supported by the generally low voltages and high currents obtained in epitaxial devices. In polycrystalline devices dislocations are unimportant because there are not a significant number of dislocations in either good or bad polycrystalline devices.

Voids

Voids were found to be common in all films including both polycrystals and single crystals. However, their density was much greater in layers deposited using a multistage process. The voids are highly faceted on (112)-type planes with both plane types (Se and metal terminated) appearing. The appearance of voids in the multistage deposited material along with analysis of epitaxial growth results shows that these are Kirkendal voids that result from coalescence of moving vacancies where a gradient in the vacancy flux is occurring locally. The presence of voids is not correlated with device performance. Indeed, it is possible that voids are actually correlated with better devices, not because the void improves the device directly but because it is a marker of moving vacancies, which may improve the device through organization of the native point defects.

Grain boundaries

As noted above, there is no obvious correlation of grain boundaries with device performance. Taking the epitaxial device results into consideration, one might even hypothesize that grain boundaries are beneficial to the device. This conclusion is described in more detail in the microchemistry section, below.

Phases and ordered defects

Cu-rich films result in a thin epitaxial layer of Cu_2Se second phase on the surface along with larger Cu_2Se precipitates. These are certainly detrimental to the device performance. However, it is less clear whether there is any negative effect due to Cu_2Se buried in the device well below the surface. Ordered defect phases, clearly visible in many epitaxial films, were not observed in polycrystalline materials based on diffractions patterns, even when the films were substantially group III-rich. There is therefore no clear evidence connecting the formation of ordered defect phases with either particularly high or low device performances.

The heterojunction and the CdS

We examined the CdS layers and their interface with the CIGS absorbers in a number of devices. The CdS was uniformly nanocrystalline with roughly equivalent grain sizes for devices from a variety of laboratories deposited under different conditions. However, the average texture of the films and the tendency to form an initial epitaxial layer on the CIGS varied somewhat. Although no trends or clear results could be obtained in the initial measurements conducted under this program, there is a possibility that the nanostructure of the heterojunction has an effect on the resulting devices. This would certainly be expected and it is somewhat surprising that there is not a more clear relationship. It is also possible that no correlation between the CdS nanostructure and the nature of the heterojunction has no effect on devices. The interface requires further study and in particular comparison of more devices from a wider variety of laboratories.

Microchemistry

The majority of the effort under this program was devoted to examination of the nanochemstry of CIGS and in particular to the heterojunction and grain boundaries. The analyses included nanoprobe EDS, angular dark field (ADF) imaging [more commonly known as Z-contrast imaging], and electron energy loss spectroscopy (EELS). We will consider the value of application of the three techniques to CIGS devices first and then what was learned from them about CIGS devices. There is considerable skepticism about nanoprobe EDS analyses and the possible experimental artifacts that could result from it so these are discussed in some detail.

Nanoprobe EDS:

This is by far the simplest and most versatile probe technique for analyzing CIGS. We used two primary TEM instruments, both highly optimized for nanoprobe EDS analysis, and both having much less than 2 nm probe diameters. The VG 501 STEM is optimized for this analysis and can conduct both point mapped and line scan analyses. The instrument has an ~1.6 nm probe beam and a cold-cathode source optimized for both small probe size and for stability. Thus individual analyses should be very comparable. The other instrument is a JEOL 2010F STEM, a state-of-the-art instrument with a 1 nm probe beam. The field-emission source is not as stable as the VG microscope source but the results were not found to be affected by source drift in the 2010F. Sample thicknesses in these analyses were reduced to <60 nm to minimize beam spreading in the sample to effectively zero.

A lattice image of a CIGS grain boundary is shown in Figure 1, along with a schematic showing the beam diameter on the same scale. The grain boundary shows a substantial width in this sample, indicating that the boundary is moving across the imaged area from the top to the bottom of the sample as indicated in the schematic. Assuming that the grain boundary is only effectively two atomic layers thick, as indicated by lattice images of well-aligned boundaries, the EDS probe should encompass a volume consisting of approximately half of the atoms in the grains and half in the grain boundary. Therefore, a change in composition of the grain boundary of ±4 at.% would be read as a variation of ±2 at.% in the nanoprobe EDS.

Another source of error in the EDS nanoprobe is counting statistics. If one counts too long, beam damage to the specimen becomes more likely. This is most likely to result in Se loss and either Cu or In accumulation. No beam damage artifacts in the compositions were observed, although visible beam damage in the image did occur if the probe was left in one location too long. The damage was probably the result of carbon contamination on the specimen surfaces as there was no composition change with beam exposure time. More serious was drift of the beam across the sample with time, especially in the 2010F. We studied the compositions measured as a function of counting time to determine the optimum time. The best compromise between noise reduction and minimizing beam drift and beam damage was found to be 50-70 sec per point in the 501 and somewhat shorter in the 2010F. To determine the noise in the EDS measurements we studied GaAs single crystals, which are known to be stoichiometric to parts per million or better. The results are shown in Figure 2. The variation is ±1.25 atomic % for each element. However, a closer examination shows that the that the data tends to drift along the line scans suggesting that the actual noise-related variation may be well below ±1 at.% and that the remainder may be due to real local variations resulting from sample preparation. In all discussions below we will assume that the "noise" is ±1.25% and that all smaller variations are

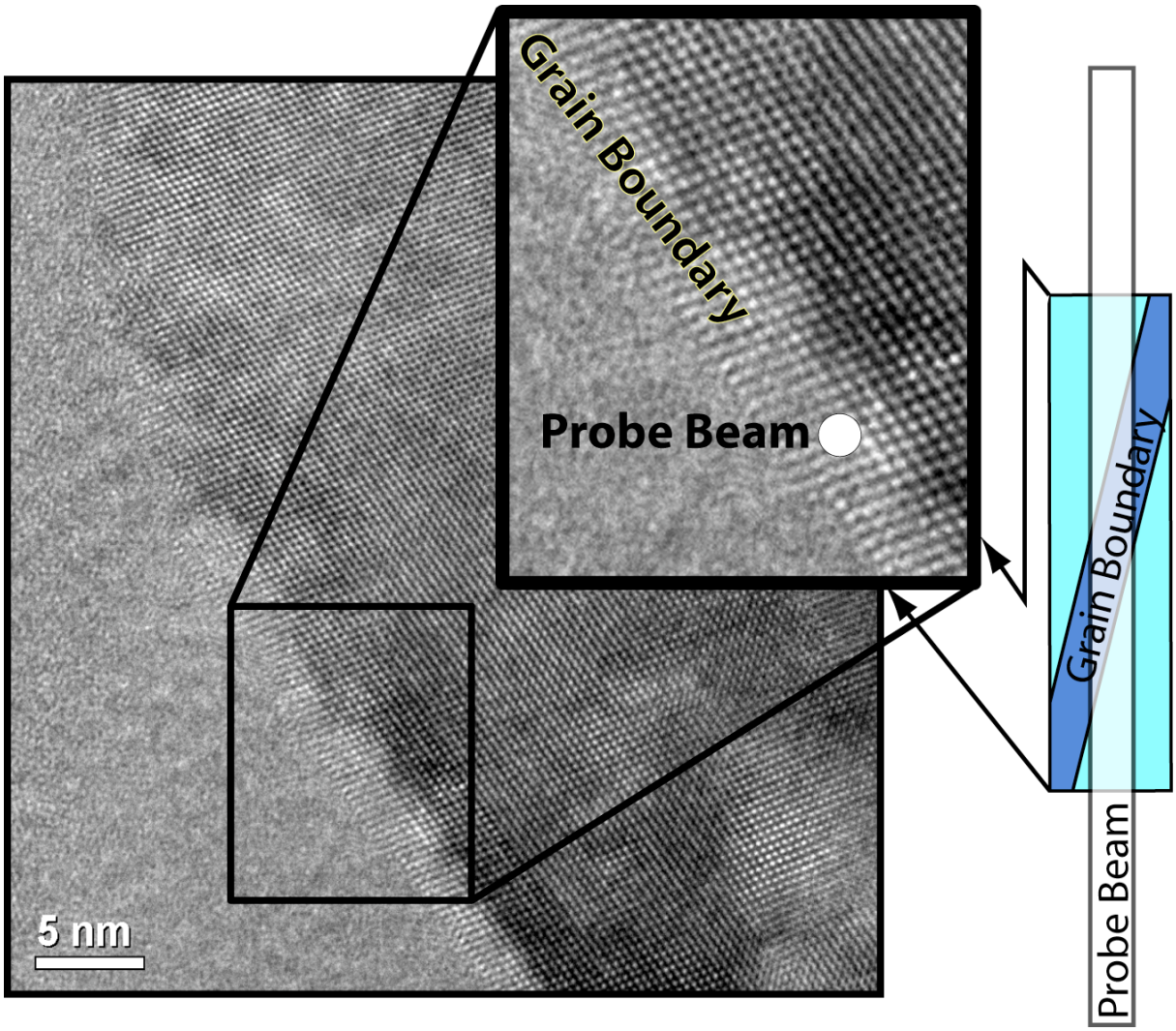

Figure 1: A lattice image of a grain boundary in an IEC CIGS film deposited at 580°C. The schematic diagram shows the analyzed area relative to the observable boundary. The box in which the grain boundary is indicated represents the estimated sample thickness relative to the beam diameter. The tilt of the grain boundary relative to the normal is determined from the image of the boundary. The circle on the lattice image shows the scale of the probe beam. Note that if the estimated thickness changed the fraction of boundary in the probed volume would not change as this would be equivalent to distorting the schematic at the right vertically without changing the horizontal dimension or beam diameter.

noise in the measurement. However, it is very likely that there are real composition fluctuations in the CIGS, as there appear to be in the GaAs standards resulting either from the sample preparation (less likely in the case of CIGS) or due to real changes in the sample locally (most likely). The reason to believe that the fluctuations are real is that the behavior above and below the ±1.25% noise level is equivalent in the CIGS. If the larger fluctuations are real (see below) then the smaller fluctuations should also exist as the data, ignoring noise, suggests.

A common argument against nanoprobe EDS is that the composition was changed as a result of sample preparation by ion beam sputtering. There are several reasons to dismiss this concern.

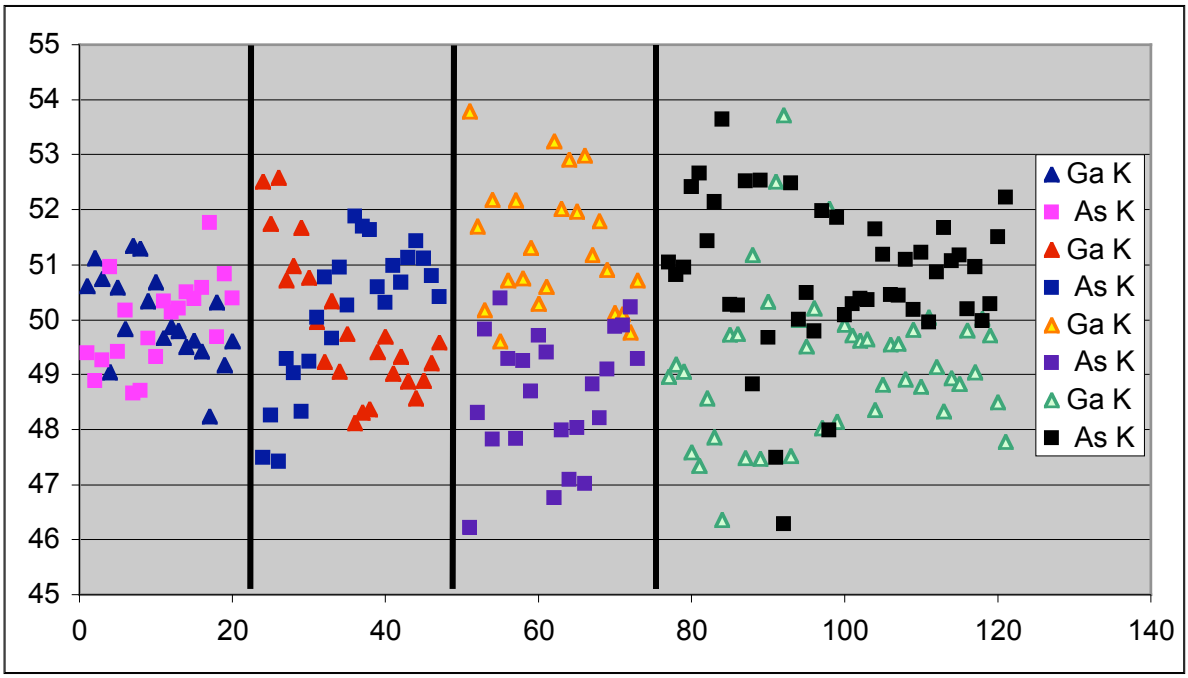

Figure 2: Shows the systematic and statistical variation in EDS analysis of GaAs wafers. Each set of data represents a different line scan obtained from a different region of the sample. Some evidence of variation of composition in thin samples may be found. For example, the second set of data in the figure (points 21-44) are from a sample that showed significant thinning across the analyzed region.

First, when samples are prepared properly no evidence for the development of surface islands (usually In) are observed. Furthermore, no systematic correlation between composition and sample thickness is observed. Samples with altered surface compositions resulting from sample preparation would exhibit composition variations directly correlated with the sample thickness as the analysis would average over relatively less surface and more bulk. Second, an altered surface layer due to sputtering would have a composition related to sputtering yields rather than bulk chemical preference. Therefore, they would tend to deviate in a systematic rather than random way in the direction of the lowest sputtering yield material. In CIGS this would tend to lead to reduction in Cu and Se with an increase in group III element. This was not observed. Finally, ion milling was carried out with liquid-nitrogen cooling to reduce diffusion to a minimum. At low temperatures only minimal surface diffusion and no bulk diffusion would be expected. As a check we compared samples prepared with and without this cooling and found no difference.

Because many of the results reported below concern grain boundaries and interfaces, we note that if the sample preparation were altering the boundary/interface composition, then again the result would be expected to be dependent on both preparation conditions and sample thickness. Furthermore, the tendency to change the boundary composition beyond the range of sputtering by diffusion would tend to take the system in the direction of equilibrium. If the sample intrinsically wanted an altered grain boundary composition, it is unlikely that a sample preparation artifact would take it away from rather than toward this condition.

We do find that the samples changed with time in air over the course of days to weeks. This was most likely due to surface oxidation. Therefore, fresh samples were prepared for each analysis.

We emphasize that we do not believe that any of the results described below were affected by sample preparation artifacts and that most of the variation in compositions measured is due to real variations in the local film composition in the nanoprobed volume (~150 nm^3). The number of atoms in such a volume is ~1500 Cu ~1500 group III atoms and ~3000 Se atoms. One atomic percent of 6000 atoms is therefore 60 atoms in the probed volume. In a material with as many point defects and defect clusters as are found in this material it would hardly be surprising to find such a level of variation or more.

Angular dark field (Z-contrast)

We have obtained several angular dark field images in the JEOL 2010F, primarily of the CIGS/CdS heterojunction. This region was chosen because for an epitaxial interface it is often difficult to tell where the chemical junction is based on the structure. The average atomic mass of CdS is 72 AMU/lattice site (112 and 32 for Cd and S) while for CIS the masses 115 (In), 63 (Cu) and 80 (Se) give an average mass/lattice site of 84.5. Therefore, the Z contrast is weak. However, we did get some good Z-contrast images. Typical examples are shown in Figure 3. However, no independent analytical results were obtained yielding answers different from other measurements. Therefore for the current project we focused more on EDS.

Electron Energy Loss Spectroscopy

We obtained energy filtered electron spectra from our CIGS samples. The results show evidence

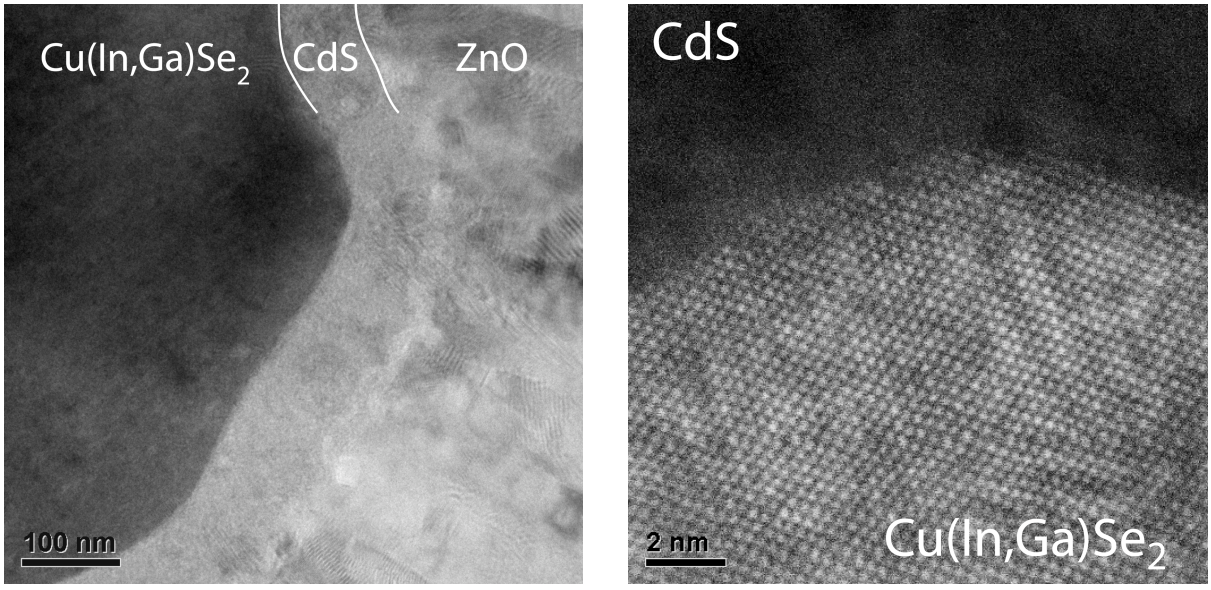

Figure 3: Z-contrast images of the CdS/CIGS junction in low and high resolution magnifications. The CdS/ZnO boundary in the low-magnification image appears tilted or rough. The bulk of the ZnO may be distinguished by its clearly columnar microstructure. Because the CdS lattice does not produce an lattice image in the high-resolution image it appears dark both because of the average Z of the material and because of the imaging conditions.

of peaks due to Cd, In, and other elements. The peak positions for these two elements are sufficiently separated that for careful choice of the energy window, it should be possible to produce an energy filtered image giving local chemistry of the interface. However, the methods require obtaining two energy filtered images at different energy and subtracting them electronically. Although this is promising, it is sufficiently complicated and the resulting images were sufficiently noisy that the simpler EDS analysis was pursued for the time this project was ongoing. However, this technique is likely to be necessary ultimately for a detailed analysis of the CdS/CIGS heterojunction and possibly the grain boundaries. We anticipate that Na and O may be especially susceptible to this method and are not easy to probe with EDS.

Microchemistry of CIGS

We present here a brief summary of the experimental results and the implications of the EDS data for devices. Details of the experiments and the data are provided in publications and in the final report of the program.

Grains and grain boundaries

No evidence of a difference in composition of grain boundaries and grains was found on average in SSI, GSE, and the high-temperature IEC CIGS device layers. Typical results are plotted on ternary phase diagrams in Figure 4 for the four IEC samples studied in greatest detail.

The plots show large scatters in the data, well above that of the noise in the analysis technique, implying that the variations in chemistry are very likely real. This is further emphasized by the relatively narrow distributions of data points in the low-temperature bilayer sample data, coupled with the systematic variation in compositions in the direction of missing group III atoms. The scatter along this trend is only of the scale of the noise circle. The data for the low-temperature bilayer film is the only result showing a strong and consistent difference between the grains and grain boundaries in the films. The best correlation of device performance with any aspect of the EDS data is with the scatter in the data relative to its average value. Because we believe that these scatters represent real variations, this means that a smaller variation represents less local chemical variation. Presumably this would correspond also to narrower Urbach edges on the bands and less carrier trapping. The composition fluctuations appear consistent with band edge fluctuations observed by photoluminescence and cathodoluminescence. We note also that the magnitude of fluctuation of the grains and grain boundaries are roughly consistent.

It is important to emphasize again -- all device layers grown at above 550°C studied here show no significant difference in grain and grain boundary chemistry. This is true for a very large collection of line scans across the boundaries. In each case an effort was made to align the probe beam directly down the boundary by appropriate tilt of the sample. Line scans were taken obliquely across the boundary rather than normal to the boundary plane to maximize the data on the boundary itself and to minimize the possibility of an accidental miss. The composition data points in the bulk and boundary show statistical fluctuations but one can not pick out the boundary point from the line scan nor do the averages differ as shown in figure 4.

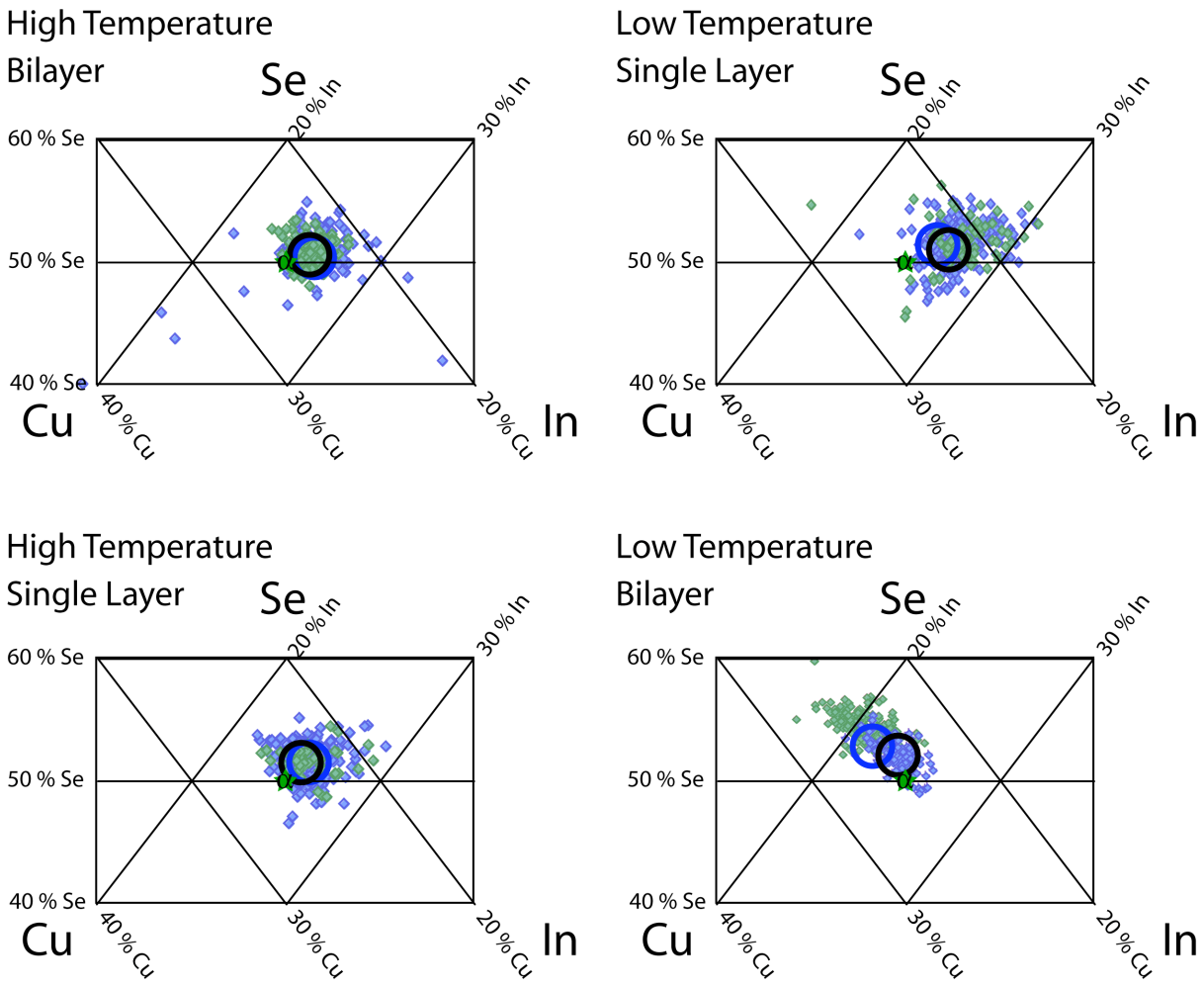

Figure 4: Nanoprobe EDS analyses of grains and grain boundaries in four IEC samples showing the similarity of the data. The two circles in each plot represent the average atomic composition of the grains (black) and grain boundaries (blue). The diameter of the circles represent the expected noise in the EDS data from the GaAs analysis (Fig 2). The efficiencies of the devices were 16.0, 15.9, 13.7, and 11.3% for the high temperature bilayer and single layer and the low temperature bilayer and single layer, respectively.

One may ask how sensitive the measurement is. The differences in the grain and grain boundary average compositions (the circle centers in Figure 4) represent approximately one atom of difference in the metal sublattices (a change of ~0.3%). Because the measurement includes the boundary as well as the grain there can be no real difference in the boundary composition on average or we would see it in the averages.

The implication is that the grain boundary potential giving rise to a barrier to hole motion described in the literature is presumably due to partial or strong pinning of the Fermi level by dangling bonds at the interface, not passivated by a change in chemistry there. This is a typical result. Explanations based on significant changes of the chemistry of the boundary are not consistent with the results we have obtained.

Finally, we turn to the low-temperature bilayer sample where the grain boundary and grain chemistries do vary significantly. We note that these samples were grown at a temperature where Cu diffusion is not capable of bringing the I/III ratio of compositions of the layers to equilibrium throughout the depth of the sample. Therefore, it is not surprising that the material is non-uniformly distributed. The grain boundaries in this sample are clearly In-deficient ($CuSe_2$-rich). However, note that the grains are also showing this trend but with a stoichiometry closer to the alpha (CIGS) phase. Whatever is happening to drive the grains to show decreases in In content is happening more strongly in the grain boundaries. Therefore, we suspect that it is not as much associated with an intrinsic behavior of the boundaries as it is associated with the deposition conditions. The higher atomic diffusivity in the grain boundaries may have simply allowed them to express this tendency more strongly than in the bulk grains.

CdS

We examined the distribution of CdS in completed devices. We found a clearly detectable CdS signal in the grain boundaries of some films where the boundary density was relatively low. The stoichiometry of this material was Cd_2S. Therefore, it appears that it was significantly S-deficient. In spite of this we found no associated change in chemistry of the boundaries when we removed the Cd and S signals from the EDS analysis. S-deficient CdS might be expected to be more strongly n-type than pure CdS or might simply be metallic. The CdS penetration into the grain boundaries was significant, probably at least to the absorption depth of most photons in the device.

We interpret these results in terms of device performance as follows. CdS is thought to dope the surface of CIGS n-type (there is at least some data showing this). If the CdS penetrates the grain boundaries and produces an n-type region in the boundaries then the device will wrap around the grains. Thus a smaller grain size is compensated by this wrapping and carrier collection would remain high. This would also be consistent with a better device performance with dip-coated CdS where penetration would presumably be higher than with evaporated material. Furthermore, it explains why the single crystalline devices do not operate well – they have only the front surface of the device for carrier collection. This explanation is simplistic certainly as it does not account for the greater degree of recombination one would expect in the wrap-around devices. This would lead to lower open-circuit voltages.

Conclusions

The conclusions of this work are that grain boundaries have unaltered chemistry relative to bulk grains in most normal device layers. The presence of O and Na in some EDS analyses does not affect this result. Further, the boundaries may contain significant CdS following dip-coating which may significantly improve the device performances relative to non-dip-coated CdS and epitaxial devices. The boundaries themselves are not detrimental to the devices. They consist largely of (112)-type close-packed facet planes which are the most stable surfaces. These are also highly inert with respect to oxidation and other reactions indicating a low intrinsic density of unpaired electrons. No extended defect is clearly correlated with device performance.

Important issues remain to be studied in the TEM in these devices and results such as the scatter in EDS data which may be correlated with device performance remain to be verified.